ISSN 1330-3651 (Print), ISSN 1848-6339 (Online)
https://doi.org/10.17559/TV-20220509122549
Preliminary communication

Influence of Variation of Cutting Speed on Wear, Cutting Forces and Tool Temperature during Performance Drilling

Patricia BONDOR*, Dan Ovidiu RUSU, Ioan Doru VOINA, Glad CONTIU, Marcel Sabin POPA

Abstract: The paper presents the results and the influence a single factor has in the drilling process. The research is focused on how modifying the cutting speed influences parameters like cutting forces, cutting temperature, tool life, wear mechanism, and chip formation. For this experiment three different cutting speeds have been tested on high-speed adapted twisted drill geometry, each of them corresponding to a certain cutting domain: 200 m/min, 165 m/min and 110 m/min. The temperature, predicted with finite element simulation (FEM), forces, wear evolution and the shape of chips have been analysed in order to prove if high speed adapted drill geometry can be used instead of an ordinary drill while performing at lower speeds. The tests certified the ability of a drill designed for high speed to process in conditions associated with lower cutting speeds, behaving similarly in all the cases.

Keywords: cutting forces; cutting tool; cutting parameter; high speed drilling; tool wear

1 INTRODUCTION

Global market competition growth demands new and various products with high requests for quality and accessible prices. In such conditions, the imperative technical problem is to create rapid, quality and low costs products [1]. The manufacturing time, price and quality of the made product depends directly on the cutting parameters. To achieve fast manufacturing process, a new type of technology was developed, namely high-speed cutting. To increase tool life in high-speed machining, numerous investigations were performed [2, 3].

This is the reason why the tools manufacturer's primary goal is to design and develop new tools capable of high-speed machining, having as a point of reference the same quality on the product achieved until now by conventional cutting regimes [4].

However, Kivak et al. [5] examined the impact of cutting parameters on tool wear, hole quality, and hole diameter circularity while drilling Inconel 718 with uncoated and coated drill bits. It was determined that at greater rotational speeds and feed rates, the hole quality and drill bit performance are very poor. Higher cutting speeds cause significant tool wear. Therefore, increasing the cutting speed was always a factor of interest and conducted to a new tools geometry which needs now to be tested in various conditions.

In the metal machining, drilling is one of the most important steps and it represents a third of all metal cutting operations [6]; consequently a study of how an HSC prototype drill performs on conventional cutting regimes generates great interest.

The key factors that affect drill tool life are relative vibrations between the tool and the workpiece, chemical reactions, chip formation and evacuation and process temperature [7, 8]. However, the most important aspects are the machining parameters such as feed rate (f) and cutting speed (Vc) [9].

Fig. 1 shows the most popular definition of the cutting speed parameters and their range transition in accordance with the workpiece material.

In this paper the conventional cutting speed for drilling in AISI 4140 type steel was established to be at 110 m/min, the transition speed range was set to 165 m/min and the high-speed cutting (HSC) range was chosen at 200 m/min, according to the Gühring tool manufacturer that provided the drills for the following tests. It is well known that larger feed rates provide a rough surface on the drilled hole, but faster cutting speeds and point angles produce a superior surface finish due to the reduced thrust force, resulting in minimal tool wear. [10, 11].

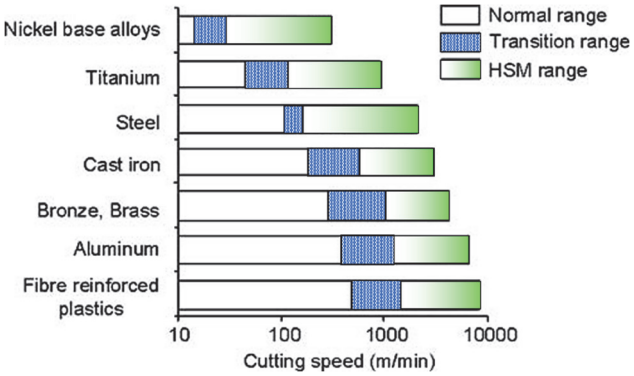

Figure 1 The Cutting speed regimes for high-speed machining (adapted after [10])

S. Dolinsek et al. [2] pointed out that the tool wear is usually caused by a combination of factors, but it is an unavoidable phenomenon of the cutting process. Tool wear appears and increases gradually or with spontaneous and drastic breakdowns. Gradual wear can occur due to chemical reactions and physical factors, and it can take two forms: wear on the tool's rake face or wear on the tool's flank. The chip leaves a crater due to the friction and adhesion on the rake face of the tool. The friction between the tool and the workpiece material, on the other hand, is the most prevalent cause of flank wear. Several forms of tool wear, which occur during high-speed cutting, are mentioned in current article.

The rake face wears mainly due to adhesion, diffusion and abrasion, while the flank face of the cutting tool wears mainly due to abrasion and oxidation [12].

The active geometry of the drill, where the wear occurs, is directly influenced by the cutting speed and was studied using FEM and SEM microscopy. The main aim of the authors' research was to observe how the cutting speed

influences the tool durability and to document the wear evolution.

For a better understanding, computer-based simulations offer the possibility to examine how different tools' cutting speeds affect the temperature value and distribution along the cutting edge. All the finite element simulations were performed using AdvantEdge software.

Temperatures between the cutting edge and workpiece material considerably affect the stress-strain relationship and result in softening the material, allowing greater deformation. The shape and location of both the primary and secondary deformation zones, maximum temperature location, heat partition and the diffusion of the tool material elements into the chip are all affected by the temperature at the tool-chip interface, which changes the friction conditions [13].

The characteristics of the mechanical and thermal loads are reflected in the chip morphology and chip formation mechanisms, which have a significant impact on premature tool failure. In the metal cutting process, a continuous saw-tooth chip appears when a relatively high cutting speed is used. When the cutting speed is further increased, chips with unusual morphologies, such as sphere-like chips and separated saw-tooth chips will appear [14].

The characteristics of chip morphology, tool life and tool wear mechanisms were further analysed for the previously mentioned cutting speeds.

The reviewed literature did not indicate that there have been any studies with tool geometries for HSC at normal cutting parameters. Most of the articles aim at increasing the cutting speed to maximize productivity.

2 EXPERIMENTAL SETUP

2.1 Workpiece Material

The drilling trials were carried out on AISI4140 (42CrMo4) tempered steel. Tab. 1 shows the chemical composition of the hardened steel under consideration.

Table 1 Chemical composition, mechanical and physical properties of quenched/tempered AISI 4140 [15]

Property	Notation	Value	Unit
Chemical composition	C	0,415	mass-%
	Si	0,40	mass-%
	Mn	0,75	mass-%
	Cr	1,05	mass-%
	Mo	0,225	mass-%
	S	0,3	mass-%
	Fe	97,13	mass-%
Young's modulus	E	204,223	MPa
Poisson ratio	v	0,3	[-]
Mass denisty	ρ	7.619×10^{-9}	ton/mm^3
Heat capacity	c_p (T ≤ 1073 K)	$200 \cdot T^2 - 65.4 \times 10^3 \cdot T + 477.04 \times 10^6$	mJ/ton/K
	c_p(T > 1073 K)	$-24.9 \times 10^3 \cdot T - 723.86 \times 10^6$	mJ/ton/K
Thermal conductivity	k	42,6	mW/mm/K
Hardness	HV	48	HRC
Initial grain size	d_0	680	nm

The steel grade AISI4140 is a heat-treatable steel with a large usage for highly stressed components that require a unique mix of high strength, wear resistance, and toughness. Heat treatable alloy steel has a tensile strength of 900-1200 N/mm^2 [16].

It is mainly used for high-toughness automotive and aeronautical components such as axle journals, gears and tyres. During the test the tested material was from a single batch.

2.2 Cutting Tool

In the experiment, a coated twist drill tool with a diameter of 6,8 mm was chosen, with a high-speed adapted geometry. The tool has a multilayer coating, and the substrate is cemented carbide with a high Cobalt concentration ratio. Carbide grain size is 0,60 µm and consists of 92% Tungsten and 8% Cobalt. The Vickers hardness of the cemented carbide lies around 1790 HV30.

Figure 2 Tested twisted drill

The tested tools are double-edged helical drills, with internal cooling and an experimental geometry optimized for cutting in the high-speed cutting range, as Fig. 2 shows.

To eliminate several factors that could influence the test results, like different carbide charges, different grinding process that includes the machine, the grinding discs or different metal coating process, all the test tools are made in the same manufacturing batch.

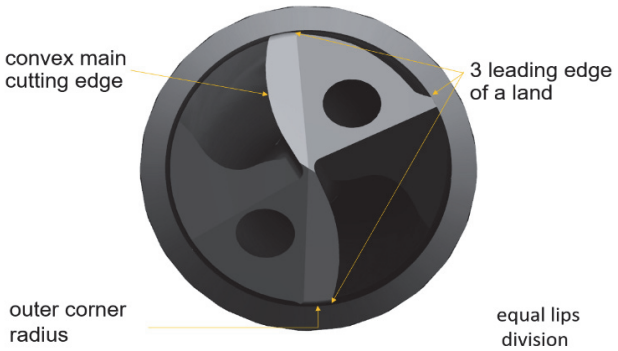

Figure 3 Main geometry aspects of the cutting tool

The drill has a convex form of the main cutting edge, as Chen and Fuh [17] demonstrated an improved cutting performance of a high-speed steel drill with curved primary cutting edges being effective in reducing the torque, the thrust force and the tool wear. The main cutting edges have equal lips division, for additional protection of external corner; the drill has a small chamfer, of 0,07 mm, at a 30° angle. For a better centring and low friction and vibration, it has three guidance facets, as shown in Fig. 3.

2.3 Cutting Tests

All the tests were performed on a 3-axis HAAS VF3-YT vertical computer numerically controlled machining centre, equipped with an ISO taper hydraulic chuck adapter, as in Fig. 4.

The maximum spindle rotation speed of the machining centre with a 15-kW drive motor is 10,000 rpm. The workpiece material was fixed in 2 precision vies, directly on the machine table.

All the drilling experiments were carried out using internal cooling with a 10% emulsion concentrate and a pressure of 40 Bar.

Figure 4 Experimental setup

Regardless of the chosen cutting speeds, the feed rate has been kept constant at a value of 0,2 mm/rot, and a machining depth of 5× nominal diameter, according to HSC catalogues of various cutting tool manufacturers [18-20]. Recommended feeds were between 0,12 and 0,35 mm/rot; in the present study, a middle value was chosen as the starting point.

The same sources indicate cutting speeds for high speed drilling of AISI 4140 starting from 160 m/min and reaching up to 200 m/min, so for this research the upper limit proposed on the market is chosen.

2.4 Experiment Equipment and Test Method

During the cutting operation, the cutting forces were monitored using a Kistler piezoelectric dynamometer (type 9129AA). It has a measuring range of ±10 kN and a measurement precision of 0,1 kN. The forces were measured on plates from the same batch of material attached to the main measuring plate of the Kistler via a machine vise.

A multichannel charge amplifier model LabAmp 5167A was used to amplify the signal generated by the dynamometer. A low-pass filter of 50 Hz was fitted to the charge amplifier in order to remove the noise and vibrations produced by the cutting process. The data sample frequency was set at 25,000 Hz. The values of the arithmetic mean for each measurement were recorded.

Furthermore, an opto-digital microscope type PG2000 was used to check and measure the overall front drill geometry wear development, like in Fig. 5. During the experiments, the drill was checked under the microscope at 25%, 50%, 75% and 100% of its expected service life, as provided by the norm VDI 3326 [21], and additionally, for a better understanding of the phenomena that have occurred, also at 30% and 60% of the durability.

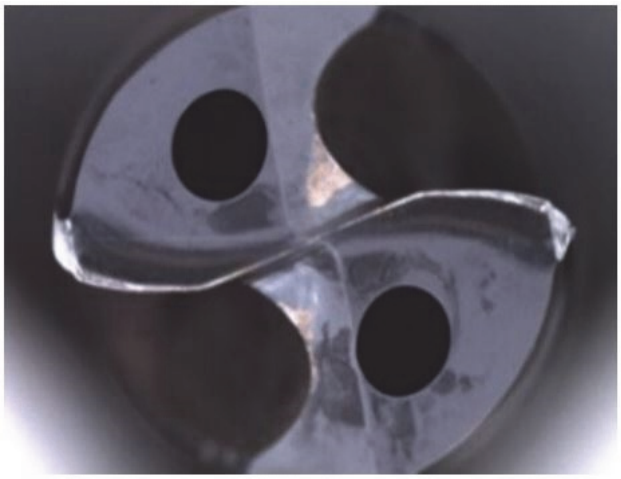

Figure 5 Wear on clearance face

The tools were also inspected and evaluated using SEM type Zeiss Sigma 300 during and after the drilling tests, at the same intervals.

Images were captured with magnifications of 75× for the overall image of the tool, 100× for the analysis of the entire chisel edge of the tool, 250× for the detailed analysis of the wear and 500× in case of special particularities.

2.5 Finite Element Simulation

The system formed by device, work tool and workpiece determines the forces and torque during the manufacturing process. In order to understand the wear process and the tool behaviour at different cutting speeds, the analysis with FEM was necessary. This research focused on the temperature distribution on the drill during the cutting process, in order to anticipate the wear mechanism associated with the temperature.

The heat transfer analysis is based on Fourier's law [22]:

$$\frac{\partial}{\partial_x}\left(\lambda\frac{\partial T}{\partial x}\right)-\rho c\frac{\partial T}{\partial t}=0 \tag{1}$$

where λ is the thermal conductivity / W/m·K; T - the temperature in / K; t - time in / s; ρ - mass density, f - the material in / kg/m$^{3;}$ c - specific heat / J/kg·K.

For the heat transfer FEM analysis, the geometric model of the cutting tool and of the workpiece was established and the thermal heat transfer was represented [22].

With more than 50000 tetrahedral pieces, the workpiece (Fig. 6) has been modelled as a plastic deformable.

The tool (Fig. 6) was created with more than 300000 elements and was designed as rigid. As a tool material, coated cemented carbide was chosen, and the thermal characteristics were acquired from the AdvantEdge material database.

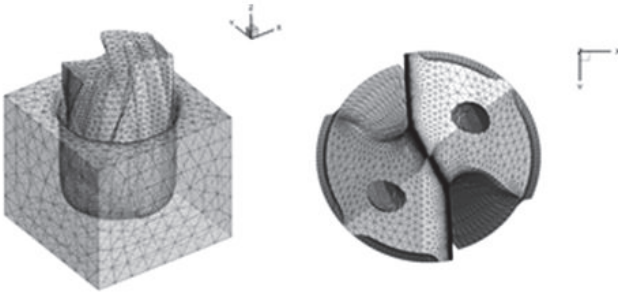

Figure 6 Geometrically rendered pattern

The cutting edge was meshed with reduced size finite elements and for the rest of the body coarse finished elements were used. For the tool the maximum element size is 1,5 mm and the minimum element size is 0,02293 mm. The finest mesh is located on the cutting-edge area. For the part, the maximum element size is 0,3 mm, while the minimum element has 0,03 mm. The resulting mesh is reproduced in Fig. 6.

As long as the feed is f = 0,2 mm/rev., the feed on the tooth (being a twisted drill-type tool with 2 cutting edges) is fz = 0,1mm. The size of the finite element must be at least 3 times smaller than the size of the chips. It follows that the minimum elements of 0,02293 mm for the tool and 0,03 mm for the workpiece are considered appropriate for the FEM analysis [23].

It is essential to remember that the research objective justifies the variation in mesh precision between the workpiece and the tool. The simulation focuses on the tool since it wants to investigate how tool wear develops. In keeping with this concept, the workpiece was modelled using a minimal number of components to decrease calculation times.

The test conditions were made at a drill depth of 1xD mm, with the feed f = 0,2 mm/rev., as in Fig. 7. The friction coefficient between the tool and the workpiece was kept as constant at the value of 0,5 [24].

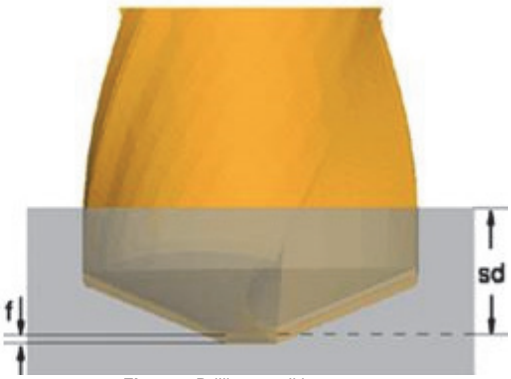

Figure 7 Drilling conditions

The properties of the processed material have been preserved as those in the data library of AdvantEdge software - AISI 4140.

3 RESULTS

The durability was given by the stopping criteria, especially by the wear width noted with VBave which was set at 200 µm, as provided by the norm VDI 3326 to be maximum 3% of the drill diameter and measured on PG2000 microscope at different intervals during the tests. The first cutting speed that reached the maximum VBave, which was Vc = 200 m/min, defines the test stop threshold and sets the maximum tool life limit (100% durability).

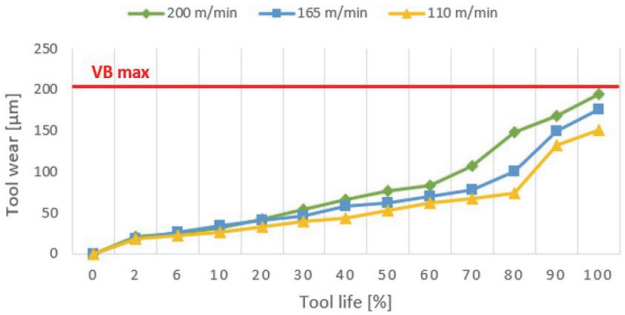

Figure 8 Tool wear chart

The test results show that all the proposed variants have reached a durability of 100%; moreover, two of them did not exceed the wear limit previously imposed. The wear was always measured on the cutting edge and clearance face.

At all cutting speeds, wear follows a predictable pattern, going through all stages of wear intervals such as: running-in wear between 0 and 20%, normal wear up to 60% and critical wear up to 100% of tool life, according to Fig. 8.

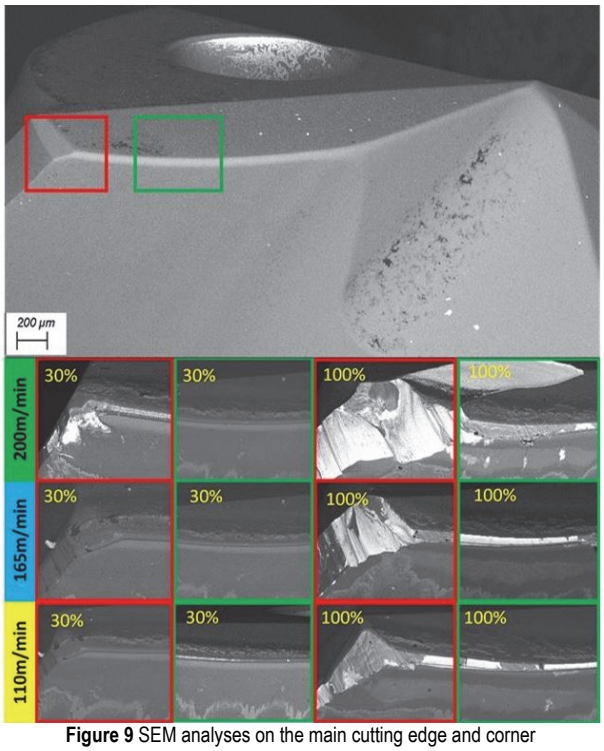

Figure 9 SEM analyses on the main cutting edge and corner

Studied under the SEM microscope, the primary wear processes of the cutting edge examined at a cutting speed of 110 m/min were adhesion, as shown in Fig. 9. At a cutting speed of 200 m/min, chipping occurred on the cutting corner, and at 110 m/min it appeared on the connection radius.

At a cutting speed of 200 m/min, the average value and amplitude of tool stress were greater, showing the combined effects of more severe heat and mechanical impact in the cutting process. Therefore, this resulted in the

appearance of chipping on the cutting corner, which was not so obvious when the tool was tested at 165 and 110 m/min. The deterioration of the tool material quality produced by high cutting temperatures and relatively strong mechanical and thermal impact at higher cutting speeds was the primary culprit.

Figure 10 Tool wear at the end of the test with a. 200 m/min; b. 165 m/min; c. 110 m/min

No tools were broken during the tests and they were not completely damaged, they can be re-sharpened and reused.

The material deposition on active geometry of the tool leads to a constant increasing evolution of torque in all tested cutting speeds in drilling process. After 40% tool durability, the torque begins a constant and linear grow till the end of the test for the HSC drilling, while in the case of transition and conventional speeds it continues to have a down/upward evolution but with small oscillations associated with material deposits, according to Fig. 10.

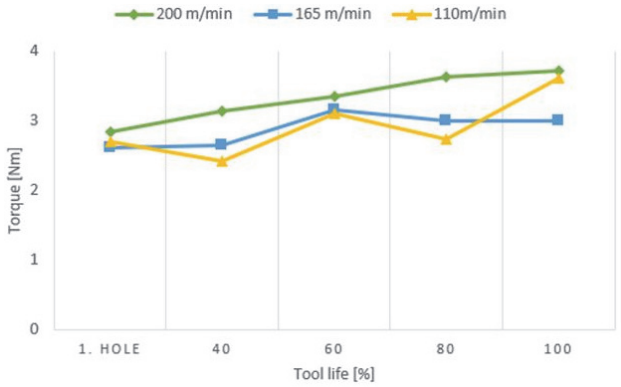

Figure 11 Torque evolution chart

At conventional and transition cutting speeds, although different parameters are used, the recorded torque shows close values.

In the case of a cutting speed of 200 m/min, the torque increases constantly with the wear. For the cutting speed of 165 m/min it is maintained at the same value up to a durability of 40%, then it increases by approx. 10% (2,75 Nm ≥ 3 Nm) until 60% durability, and then it follows a slightly downward trend. For the cutting speed of 110 m/min the value of the torque decreases to a durability of 40% by approx. 10% (2,75 Nm ≥ 2,5 Nm), then it increases by approx. 20% when the drill reaches a tool life of 60%, so that at 80% of its lifetime it will reach the value from the beginning and at the end it will have an increase of approx. 28% of the initial value. Although the torque values do not differ significantly in the case of the 3 parameters, it can be seen from Fig. 11 that lower speeds also generate lower torques.

The results show that the macrogeometry and sizing of the drill core do not exceed the limits at which the drill must operate.

At a speed of 200 m/min, the FEM simulations certify a higher temperature in the corner area that translates into a pronounced wear in that zone. At the other two speed ranges, the heat is evenly distributed along the cutting edge and the temperature has lower values. The even temperature distribution along the main lip is considered the main reason for a uniform wear.

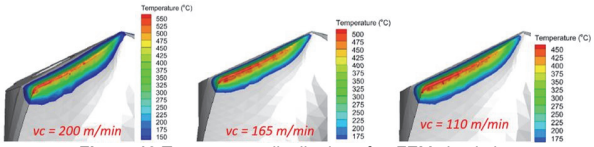

Figure 12 Temperature distribution after FEM simulation

In Fig. 12 the simulation is performed in ideal conditions, with the edges and surfaces ideally coated. After the appearance of wear (around the durability that reached 30%), the simulated model no longer reflects the reality considering the thinning of the coating, material deposition and the modification of the microgeometry of the main lip and respectively of the drill corner.

The temperature at cutting speed of 110 m/min, even if it is distributed relatively evenly along the entire length of the edge, has high values, close to 450 °C. At the highest cutting speed, the highest temperature is in the corner of the drill and reaches up to 550 °C, which facilitates the appearance of wear.

The transition speed reaches a temperature of 500 °C and it is distributed along the entire cutting length.

The temperature is a result of the intense processes of friction between the tool, the chip and the piece, respectively of the plastic deformation of the detached chip.

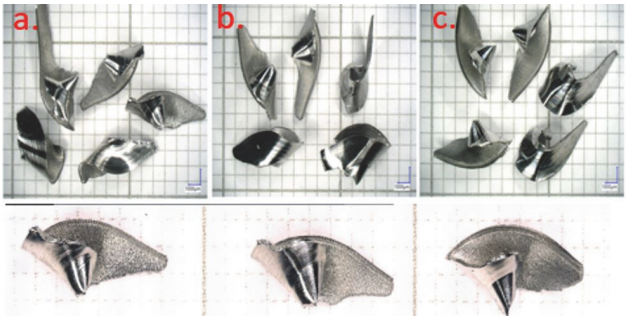

Figure 13 Chip form at a. 200 m/min; b. 165 m/min; c. 110 m/min

During the FEM simulations, the chip formation was also observed, and it coincides with the shape and geometry of the chips taken as a result of the cutting process.

The geometry of the formed chips is similar, regardless of the cutting speed. The chips are fragmented and relatively easy to evacuate, with a similar appearance according to Fig. 13. The shear zones are much more obvious in the case of chips obtained with a speed of 200 m/min, compared to 110 m/min.

4 DISCUSSIONS

It has been found that in the running-in and normal wear domain, for all the cutting regimes, VBave has a constant growth and reaches a value between 60 and 70 μm.

After this interval, the VBave increases rapidly in the case of the cutting regime with a speed of 200 m/min, during the critical wear, it reaches the following values: at a durability of 70% - VBave = 100 μm; 80% - VBave = 150 μm; 90% - VBave = 165 μm later reaching the maximum set of VBave = 200 μm.

The same phenomenon does not happen in the case of lower speeds where the upper limit of the normal wear is reached at 70% of tool life in the case of the transition speed and at 80% in the case of the conventional cutting speed. Both regimes with cutting speeds under the HSC range tend to have a sharp growth of the wear width when approaching 90% durability, reaching VBave of 150 μm in the case of transition speed and 140 μm in the case of conventional speed. However, none of the drills that were tested with conventional and transitional parameters have reached the maximum imposed limit of 200 μm VBave.

Even if the conventional speed represents only 55% of the speed from the HSC range, the temperature was reduced by only 20%. This difference influences the temperature distribution on the active geometry of the drill and leads to a less accentuated wear during the tests and evenly distributed (Fig. 9 and Fig. 13). The temperature decrease is not directly proportional to the speed decrease.

5 CONCLUSIONS

Considering the comprehensive experimental research in which more than 100 measurements were performed, and the results that followed and confirmed the theoretical investigations and finite element simulations, the following may be concluded:

In the case of conventional and transition cutting speeds, the wear has a constant increase until the tool life reaches 80% and 70% respectively, after these thresholds it goes into an extreme growth.

The tested drills with conventional cutting speed, at the end of the durability tests have a wear width VBave = 150 μm equivalent to the wear width of the drills tested with 200 m/min at a tool life of 80%.

Decreasing the cutting speed reduces the drill wear in the corner of the tool. According to Fig. 11, the wear range narrows from the tool corner to the top, remaining predominantly in the transition radius area, as the cutting speed decreases.

The wear size directly influences the torque; when the tools were new, the value of the torque was not significantly influenced by the cutting speeds.

The torque values do not differ significantly in the case of the 3 parameters; it can be seen from diagram 12 that lower speeds also generate lower torques.

The maximum temperature varies by up to 100 °C between the HSC and the conventional speed, which is shown in the FEM Simulations.

The chip serration became more noticeable as the cutting speed rose, according to the FEM Simulations and experimental analysis. The cutting speed did not influence the chip evacuation, they kept the shape and curvature.

This study confirms that the drills with adaptive HSC geometry can also operate at speeds lower than high speed machining and can be used on machines that do not reach such high performances.

The main objective of the research was achieved by demonstrating that the new geometries adapted for HSC can operate smoothly even at conventional cutting speeds.

Acknowledgements

This work was supported by the European Development Fund and the Romanian Government through the Competitiveness Operational Programme 2014-2020, project ID P 34 466, MySMIS code 121349, contract no.5/05.06.2018. The authors are also grateful to the Gühring Company for the technical and logistical support.

6 REFERENCES

[1] Čekić, A., Begić-Hajdarević, D., & Kulenović, M. (2013). Effect of the cutting parameters on cutting forces in high speed face milling. *Technical Gazette*, *20*(5), 775-780.

[2] Dolinšek, S., Šuštaršič, B., & Kopač, J. (2001). Wear mechanisms of cutting tools in high-speed cutting processes. *Wear*, *250*(1), 349-356. https://doi.org/10.1016/S0043-1648(01)00620-2

[3] Fang, N. & Wu, Q. (2009). A comparative study of the cutting forces in high speed machining of Ti-6Al-4V and Inconel 718 with a round cutting edge tool. *Journal of Materials Processing Technology*, *209*(9), 4385-4389. https://doi.org/10.1016/j.jmatprotec.2008.10.013

[4] Tonshoff, H. K. I., Konig, I., Neises, A., & Aachen, R. (1994). *Machining of Holes Developments in Drilling Technology*, *43*, 551-561.

[5] Kivak, T., Habali, K., & Seker, U. (2012). The effect of cutting paramaters on the hole quality and tool wear during the drilling of inconel 718. *Gazi University Journal of Science*, *25*(2), 533-540.

[6] Chen, W.-C. & Tsao, C.-C. (1999). Cutting performance of different coated twist drills. *Journal of Materials Processing Technology*, *88*(1), 203-207. https://doi.org/10.1016/S0924-0136(98)00396-3

[7] Matsumura, T., Hori, I., & Shirakashi, T. (2010). Analysis of cuttinng temperature in drilling process. *International Journal of Material Forming*, *3*(SUPPL. 1), 499-502. https://doi.org/10.1007/s12289-010-0816-y

[8] Khan, S. A., Shamail, S., Anwar, S., Hussain, A., Ahmad, S., & Saleh, M. (2020). Wear performance of surface treated drills in high speed drilling of AISI 304 stainless steel. *Journal of Manufacturing Processes*, *58*(October), 223-235. https://doi.org/10.1016/j.jmapro.2020.08.022

[9] Prasad, B. S. & Sai Ravi Kiran, D. S. (2019). Experimental investigation to optimize tool performance in high-speed drilling: a comparative study. *Journal of the Brazilian Society of Mechanical Sciences and Engineering*, *41*(11), 535. https://doi.org/10.1007/s40430-019-2049-4

[10] Samy, G. S. & Kumaran, S. T. (2017). Measurement and analysis of temperature, thrust force and surface roughness in drilling of AA (6351)-B4C composite. *Measurement*, *103*, 1-9. https://doi.org/10.1016/j.measurement.2017.02.016

[11] Yardimeden, A., Kilickap, E., & Celik, Y. H. (2014). Effects of Cutting Parameters and Point Angle on Thrust Force and Delamination in Drilling of CFRP. *Materials Testing*, *56*(11-12), 1042-1048. https://doi.org/10.3139/120.110666

[12] Majerík, J., Barényi, I., Pokorný, Z., Sedlák, J., Neumann, V., Dobrocký, D., Jaroš, A., Krbaťa, M., Jambor, J., Kusenda, R., Sagan, M., & Procházka, J. (2021). Analysis of the OCHN3MFA steel in terms of cutting forces and cutting material flank wear mechanisms in hard turning processes. *Bulletin of the Polish Academy of Sciences: Technical Sciences*, *69*(6), e139203-e139203. https://doi.org10.24425/bpasts.2021.139203

[13] Abukhshim, N. A., Mativenga, P. T., & Sheikh, M. A. (2006). Heat generation and temperature prediction in metal cutting: A review and implications for high speed machining. *International Journal of Machine Tools and Manufacture*,

46(7), 782-800. https://doi.org/10.1016/j.ijmachtools.2005.07.024
[14] Cui, X., Zhao, B., Jiao, F., & Zheng, J. (2016). Chip formation and its effects on cutting force, tool temperature, tool stress, and cutting edge wear in high- and ultra-high-speed milling. *The International Journal of Advanced Manufacturing Technology*, *83*(1), 55-65. https://doi.org/10.1007/s00170-015-7539-7
[15] Buchkremer, S. & Klocke, F. (2017). Modeling nanostructural surface modifications in metal cutting by an approach of thermodynamic irreversibility: Derivation and experimental validation. *Continuum Mechanics and Thermodynamics*, *29*(1), 271-289. https://doi.org/10.1007/s00161-016-0533-y
[16] EN 10083-3-2006 (DIN EN ISO 683-2).
[17] Chen, W. C. & Fuh, K. H. (1995). The cutting performance of a TiN-coated drill with curved primary cutting edges. *Journal of Materials Processing Tech.*, *49*(1-2), 183-198. https://doi.org/10.1016/0924-0136(94)01326-V
[18] Mitsubishi Materials. (2007). *WSTAR DRILL catalog*.
[19] Mapal. (2022). *Bore machining catalog*.
[20] Sandvick Coromat. (2020). *Vollhartmetall-Werkzeuge Katalog*.
[21] Vollhartmetall-bohrwerkzeuge, P. (2002). *INGENIEURE VDI 3326*, 1-8.
[22] Liu, Y. (2019). Heat transfer for high temperature operation based on ANSYS thermal analysis. *AIP Conference Proceedings*, *2122*(July). https://doi.org/10.1063/1.5116485
[23] Uçak, N., Çiçek, A., Oezkaya, E., & Aslantas, K. (2019). Finite element simulations of cutting force, torque, and temperature in drilling of Inconel 718. *Procedia CIRP*, *82*, 47-52. https://doi.org/10.1016/j.procir.2019.03.277
[24] Bowden, F. P., Bowden, F. P., & Tabor, D. (2001). *The Friction and Lubrication of Solids* Clarendon Press. https://books.google.ro/books?id=OQ7FCKNixK0C

Contact information:

Dan Ovidiu RUSU, PhD Student
(Corresponding author)
Department of Manufacturing Engineering, Faculty of Industrial Engineering, Robotics and Production Management, Technical University of Cluj-Napoca,
B-dul Muncii nr. 103-105, 400641 Cluj-Napoca
E-mail: dan.rusu@tcm.utcluj.ro

Patricia BONDOR, PhD Student
Department of Manufacturing Engineering, Faculty of Industrial Engineering, Robotics and Production Management, Technical University of Cluj-Napoca,
B-dul Muncii nr. 103-105, 400641 Cluj-Napoca
E-mail: patricia.bondor@tcm.utcluj.ro

Ioan Doru VOINA, PhD Student
Department of Manufacturing Engineering, Faculty of Industrial Engineering, Robotics and Production Management, Technical University of Cluj-Napoca,
B-dul Muncii nr. 103-105, 400641 Cluj-Napoca
E-mail: ioan.voina@tcm.utcluj.ro

Glad CONTIU, Professor
Department of Manufacturing Engineering, Faculty of Industrial Engineering, Robotics and Production Management, Technical University of Cluj-Napoca,
B-dul Muncii nr. 103-105, 400641 Cluj-Napoca
E-mail: glad.contiu@tcm.utcluj.ro

Marcel Sabin POPA, Professor
Department of Manufacturing Engineering, Faculty of Industrial Engineering, Robotics and Production Management, Technical University of Cluj-Napoca,
B-dul Muncii nr. 103-105, 400641 Cluj-Napoca
E-mail: marcel.popa@tcm.utcluj.ro